AMERICAN SOCIETY FOR MICROBIOLOGY | Infection and Immunity®

BACTERIAL INFECTIONS

Analysis of *Staphylococcus aureus* Transcriptome in Pediatric Soft Tissue Abscesses and Comparison to Murine Infections

K. Moffitt,[a,c] E. Cheung,[a] T. Yeung,[a] C. Stamoulis,[b,c] R. Malley[a,c]

[a]Division of Infectious Diseases, Boston Children's Hospital, Boston, Massachusetts, USA
[b]Division of Adolescent Medicine, Boston Children's Hospital, Boston, Massachusetts, USA
[c]Department of Pediatrics, Harvard Medical School, Boston, Massachusetts, USA

C. Stamoulis and R. Malley contributed equally to this work.

ABSTRACT A comprehensive understanding of how *Staphylococcus aureus* adapts to cause infections in humans can inform development of diagnostic, therapeutic, and preventive approaches. Expression analysis of clinical strain libraries depicts *in vitro* conditions that differ from those in human infection, but low bacterial burden and the requirement for reverse transcription or nucleic acid amplification complicate such analyses of bacteria causing human infection. We developed methods to evaluate the mRNA transcript signature of *S. aureus* in pediatric skin and soft tissue infections (SSTI) directly *ex vivo*. Abscess drainage from 47 healthy pediatric patients undergoing drainage of a soft tissue infection was collected, and RNA was extracted from samples from patients with microbiologically confirmed *S. aureus* abscesses (42% due to methicillin-resistant *S. aureus* [MRSA]). Using the NanoString platform and primers targeting *S. aureus* mRNA transcripts encoding surface-expressed or secreted proteins, we measured direct counts of 188 *S. aureus* mRNA transcripts in abscess drainage. We further evaluated this mRNA signature in murine models of *S. aureus* SSTI and nasal colonization where the kinetics of the transcriptome could be determined. Heat maps of the *S. aureus* mRNA signatures from pediatric abscesses demonstrated consistent per-target expression across patients. While there was significant overlap with the profiles from murine SSTI and nasal colonization, important differences were noted, which can inform efforts to develop therapeutic and vaccine approaches.

KEYWORDS *Staphylococcus aureus*, gene expression, pediatric infectious disease, soft tissue infection

Staphylococcus aureus is one of the most common causes of bacterial infections worldwide. In addition to causing invasive infections, *S. aureus* is responsible for up to 75% of skin and soft tissue infections (SSTI) (1). SSTI account for millions of emergency department visits each year in the United States, and the percentage of soft tissue infections complicated by abscess formation has been rising over the last decade (2, 3). Treatment of these infections typically includes abscess drainage and antibiotics, and increasing rates of community-acquired methicillin-resistant *S. aureus* (CA-MRSA) SSTI over the last 2 decades have limited antibiotic treatment options for these infections.

A vaccine that protects against *S. aureus* infections, including SSTI, would have a major impact on health care in the United States and worldwide, but a number of challenges impede *S. aureus* vaccine development. The mechanisms of immunity are not well understood and likely vary across types of infection (4). Furthermore, *S. aureus* elaborates several toxins and antigens that facilitate evasion of host immune responses

Citation Moffitt K, Cheung E, Yeung T, Stamoulis C, Malley R. 2021. Analysis of *Staphylococcus aureus* transcriptome in pediatric soft tissue abscesses and comparison to murine infections. Infect Immun 89:e00715-20. https://doi.org/10.1128/IAI.00715-20.

Editor Andreas J. Bäumler, University of California, Davis

Address correspondence to K. Moffitt, Kristin.moffitt@childrens.harvard.edu.

Received 12 January 2021
Accepted 14 January 2021
Accepted manuscript posted online 1 February 2021
Published 17 March 2021

(5, 6). Several *S. aureus* immunization approaches have been evaluated in humans based on promising studies in animal models. These include passive and active immunization strategies, with single proteins and combinations of capsular polysaccharides and protein as antigens. However, all these approaches have failed in clinical trials (7, 8). Species-specific differences in susceptibility to infection and in vaccine-elicited immune responses likely contributed to these failures that were not predicted by the preclinical studies. In addition, a better understanding of the expression profile of *S. aureus* in the context of human infection would greatly inform the development of effective vaccine approaches.

High-throughput gene expression analysis of pathogens causing human infection has been limited by several features inherent to the composition of human infection samples and the technical requirements of various expression analysis platforms. In clinical infection samples, pathogen RNA content is about 2 orders of magnitude lower than host RNA content, and detection of relatively low-abundance prokaryotic RNA transcripts often requires deletion of eukaryotic RNA and/or enrichment of prokaryotic RNA (9). Furthermore, high-throughput RNA analysis methods such as transcriptome sequencing (RNA-Seq) and microarray rely on reverse transcription for creation of cDNA libraries, steps where bias has been shown to be introduced (10–12).

In this study, we analyzed the mRNA signature of *S. aureus* directly in pediatric abscesses. We performed direct counting of mRNA transcripts using a platform that requires no reverse transcription or RNA enrichment or depletion (13) and analyzed the *S. aureus*-specific mRNA profile from pediatric abscess drainage. Despite variability of enrolled patients' clinical features and in the composition of etiologic *S. aureus* strains, a relatively consistent mRNA signature emerged, including transcripts of well-characterized virulence factors and other proteins not previously described or of unknown function. The bacterial expression profile during infection demonstrated striking differences compared to the profile from the same *S. aureus* isolate grown *in vitro*, underscoring the importance of pathogen expression analyses directly from infected samples. We also evaluated the transcriptomic profile from *S. aureus* in the context of murine models of *S. aureus* SSTI and nasal colonization. The mRNA profile in human and murine SSTI largely overlapped, but with important differences which raise issues regarding the use of murine models for the selection of potential vaccine candidates. In light of the poor predictive record of animal models previously used to select past *S. aureus* vaccine candidates, studies such as this one to evaluate a pathogen's expression profile at the interface of human infection could better inform the development of preventive and treatment interventions.

RESULTS

Pediatric SSTI patients. We enrolled 235 otherwise healthy pediatric patients presenting with a soft tissue abscess requiring incision and drainage. Of those, 149 patients (63%) had culture-proven *S. aureus* SSTI, with 81 abscesses (54.4%) due to MRSA and 68 (45.6%) due to methicillin-susceptible *S. aureus* (MSSA). RNA was extracted from the abscess drainage of all patients with *S. aureus* SSTI; 47 of these samples yielded high-quality RNA for analysis. The clinical characteristics for the evaluable patients and multilocus sequence type (MLST) of corresponding *S. aureus* strains are described in Table 1. MRSA caused 43% of evaluable SSTI, and most of these (14 of 20; 70% of MRSA) were sequence type 8 (ST8), consistent with the USA300 strain responsible for most CA-MRSA infections in the United States (14, 15). While the majority of MSSA strains were also ST8 (17 of 27; 63% of MSSA), there was more heterogeneity in the STs of MSSA strains. Patients presented at a mean of 3.2 days of symptoms (range, 1 to 7 days) and were of mean age 11 years. At enrollment, 26% of patients were on antibiotics and 26% of patients had a history of prior SSTI. We had originally intended to evaluate the transcriptome of *S. aureus* in the nasopharynx of subjects; however, the burden of nasal *S. aureus* carriage was below the limit required for expression analysis directly from nasal swabs.

TABLE 1 Clinical demographics of evaluable patients ($n = 47$)

Parameter	Value(s)
Median age (IQR[a]), yrs	11.8 (12.9)
Ratio of males to females, no. (%)	20 (42.6)/27 (57.4)
No. (%) with MRSA	20 (42.6)
Multilocus sequence type (MLST)	MRSA ($n = 19$[b]), 14 ST8, 2 ST1472, 1 ST4080, 1 ST3624, 1 ST88; MSSA ($n = 27$), 16 ST8, 3 ST152, 2 ST30, 1 ST25, 1 ST1, 1 ST97, 1 ST 2066, 1 ST5, 1 ST3425
Median no. of days of symptoms (IQR)	3.0 (2.0)
No. (%) with fever	7 (14.9)
No. (%) with antibiotic use at time of drainage	12 (25.5)
No. (%) with history of prior abscesses	12 (25.5)

[a]IQR, interquartile range.
[b]The isolate from one evaluable MRSA SSTI was not available.

Validation of expression analysis methods. Using NanoString nCounter gene expression technology (NanoString Technologies, Seattle, WA), we custom-designed primer sets for *S. aureus* transcript quantification directly from clinical infection samples as had been done effectively for several other pathogens from human samples (16, 17). We evaluated the mRNA signature of 188 distinct transcripts that are highly conserved across *S. aureus* strains, including 169 genes with a signal sequence for surface expression or secretion and 19 additional transcripts of interest for their possible role in virulence or as immunogens (18). RNA from infection samples were hybridized with *S. aureus* target primers (see Table S1 in the supplemental material). Biological and technical variability of this method was tested. Transcript counts from RNA from separate cultures of MRSA grown to mid-logarithmic phase on different days were strongly correlated (Fig. S1A; Spearman's rho = 0.93), as were counts from the same RNA hybridized in separate reactions (Fig. S1B; Spearman's rho = 0.99), suggesting high reproducibility of the results. Specificity was also evaluated by performing expression analysis of RNA from samples obtained from patients with abscesses due to other bacteria. Transcript counts from RNA extracted from abscess samples that grew *Actinomyces* species, coagulase-negative staphylococci, or *Streptococcus pyogenes* were at background-level counts of no-RNA control hybridizations (Fig. S2).

Having validated these methods, we evaluated the transcript profile of *S. aureus* first in pediatric abscesses and then in a mouse model of SSTI to see how well the two expression profiles matched to determine whether such a model would be a valid tool for assessing the effect of genes identified as upregulated in humans. Lastly, given the inability to obtain sufficient RNA to perform expression analysis of *S. aureus* colonizing the nares of pediatric abscess patients, we developed a murine nasal colonization model that allowed a transcriptomic analysis during early establishment of carriage in mice.

***S. aureus* transcript signature in pediatric SSTI.** To account for variation in the amount of *S. aureus* mRNA present in total RNA added, transcript counts from each sample were normalized to the median transcript count from that sample. Normalized counts of each of the 188 *S. aureus* transcripts are shown for all 47 evaluable SSTI samples in the heat map in Fig. 1A; see Table S2 for a list of aggregate medians for all 188 transcripts evaluated. Despite the variability in the patient characteristics and causative *S. aureus* strains, the mRNA expression profile was very consistent across patients. High expression transcripts were similar across the majority of samples. Similarly, those transcripts with low expression had low transcript counts across the majority of samples, suggesting stable expression of the measured *S. aureus* transcripts in pediatric abscesses.

The *S. aureus* isolate from each subject's abscess was also cultured, and RNA was extracted from mid-logarithmic-phase growth and evaluated using the same expression analysis methods. mRNA counts from these *in vitro*-regrown clinical isolates are

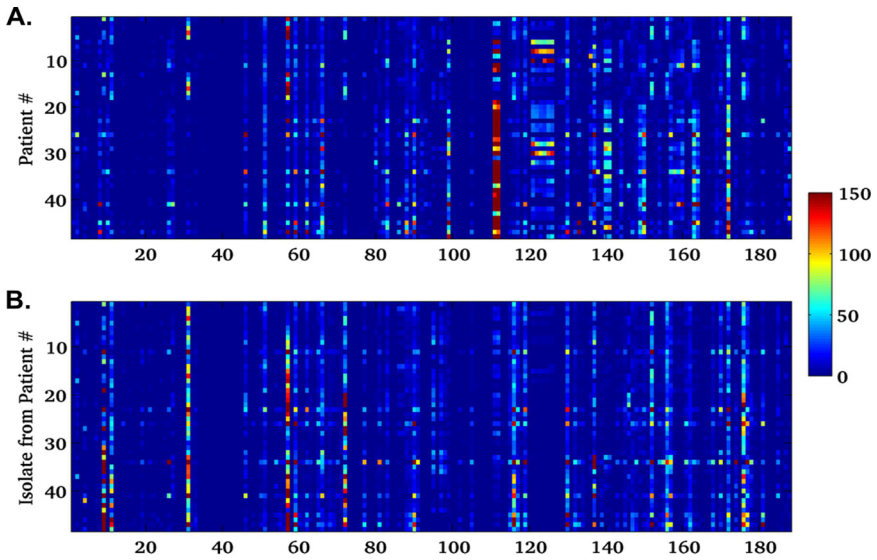

FIG 1 *S. aureus* mRNA profile in pediatric SSTI differs from that of corresponding strains regrown *in vitro*. (A) Heat map of 188 *S. aureus* mRNA transcripts (*x* axis) from pediatric abscess drainage of 47 patients (*y* axis). (B) Heat map of the same 188 transcripts from the *S. aureus* strains isolated from the 47 abscesses evaluated for panel A. Each strain was grown to mid-logarithmic phase and lysed for RNA extraction. Raw transcript counts in each sample were normalized to the median target count for that sample.

shown in the heat map in Fig. 1B. Again, the mRNA signature was highly consistent across isolates. The transcript profile of the *in vitro*-regrown isolates was very different from that obtained directly from abscesses, as shown by the scatterplot of the medians for each transcript *in vivo* in infection versus *in vitro* in regrown abscess isolates (Fig. S3), further supporting the need to evaluate gene expression *in vivo*.

Genes whose expression abundance was in the top quartile of the mRNA transcripts in pediatric abscesses are ranked highest to lowest in Table 2. Among the highest expressed transcripts were those encoding the two subunits of the Panton-Valentine leukocidin (PVL; *LukS-PV* and *LukF-PV*) and alpha hemolysin (*hla*), toxins for which there is strong evidence of a role in the pathogenesis of *S. aureus* SSTI (19, 20). Expression of other cytolysins encoded by *S. aureus*, such as gamma hemolysin (subunits *hlgB/C/A*) and leukocidin AB (LukAB, also known as LukGH), was also enriched in pediatric abscesses relative to other transcripts (21). Upregulation of these virulence factors in the abscess environment corroborates what is known about the accessory gene regulator (*agr*)-mediated quorum-sensing regulatory mechanism in *S. aureus* that increases expression of secreted toxins and virulence factors during the transition from exponential to stationary growth phase *in vitro* (22). In addition, our analysis identified several upregulated genes encoding transporter complex subunits and proteins of unknown function.

Analysis of expression data as a function of clinical and demographic characteristics. Individual transcript counts in pediatric SSTI were analyzed as a function of demographic and clinical variables. In univariate models adjusted for false-discovery rate (FDR) (23), methicillin susceptibility was significantly associated with only two transcript expression levels (USA300HOU_0031;*mecA* and USA300HOU_0078;nickel/peptide ABC transporter ATP-binding protein). Days of symptoms was significantly associated with only 2 transcript levels and marginally associated with an additional 30 transcript levels. However, in multivariate models that included both methicillin susceptibility and days of symptoms, all associations with days of symptoms were no longer significant, suggesting that the associations in univariate models testing the effect of days of symptoms were spurious and accounted for the confounding effect of methicillin susceptibility. In contrast, the significant associations between methicillin susceptibility and *mecA* and USA300HOU_0078 remained significant in multivariate

TABLE 2 Top quartile of targets in pediatric abscesses[a]

Transcript no.	Locus ID	Corresponding protein	Gene designation	Median in pediatric SSTI	Rank murine SSTI, day 3	Rank murine nares, day 3	Rank in mid-log growth USA300
112	USA300HOU_1431	Panton-Valentine leukocidin subunit S	*LukS-PV*	175.1	12	17	5
111	USA300HOU_1430	Panton-Valentine leukocidin subunit F	*LukF-PV*	143.35	14	22	7
172	USA300HOU_2564	Immunodominant antigen A	*isaA*	56.321	10	4	12
163	USA300HOU_2457	Oligopeptide ABC transporter membrane protein		34.188	3	36	82
99	USA300HOU_1099	Alpha hemolysin	*hla*	27.914	17	35	8
66	USA300HOU_0731	Hypothetical protein		27.672	11	20	15
137	USA300HOU_1946	Hypothetical protein		25.229	18	11	1
51	USA300HOU_0465	LysM family autolysin	*sle1*	24.82	31	24	35
151	USA300HOU_2285	Secretory antigen	*SsaA*	22.611	69	8	91
140	USA300HOU_2011	Leukocidin subunit	*LukB(G)*	21.32	5	80	38
165	USA300HOU_2458	Oligopeptide ABC transporter substrate-binding protein		20.495	9	53	95
141	USA300HOU_2013	Leukocidin subunit	*LukA(H)*	19.793	8	114	41
90	USA300HOU_1007	Hypothetical protein		18.525	20	14	24
150	USA300HOU_2280	Secretory antigen	*SsaA2*	17.713	53	18	111
57	USA300HOU_0619	Hypothetical protein		16.906	1	5	2
121	USA300HOU_1801	Serine protease	*SplF*	16.52	47	56	43
130	USA300HOU_1833	Peptidylprolyl isomerase	*prsA2*	16.144	23	44	22
83	USA300HOU_0939	Extracellular adherence protein	*Eap*	15.343	32	3	10
59	USA300HOU_0651	ABC transporter ATP-binding protein	*MntC*	14.341	27	10	30
126	USA300HOU_1806	Serine protease	*SplA*	12.465	77	94	55
158	USA300HOU_2401	Immunoglobulin G-binding protein	*SBI*	12.329	28	77	37
62	USA300HOU_0686	LysM domain-containing protein		12.25	49	9	49
88	USA300HOU_0997	Bifunctional *N*-acetylmuramoyl-L-alanine amidase	*atl*	12.108	41	28	47
161	USA300HOU_2405	Gamma hemolysin component B	*hlgB*	11.083	7	88	93
125	USA300HOU_1805	Serine protease	*SplB*	11.08	73	83	53
145	USA300HOU_2169	Iron (Fe^{3+}) ABC transporter binding protein		10.286	16	26	90
119	USA300HOU_1725	Catabolite control protein A	*ccpA*	9.5161	40	12	27
123	USA300HOU_1803	Serine protease	*SplD*	8.5719	72	131	58
160	USA300HOU_2404	Gamma hemolysin component C	*hlgC*	8.2186	15	97	99
46	USA300HOU_0437	Hypothetical protein		7.9363	24	1	11
117	USA300HOU_1636	Bifunctional preprotein translocase subunit	*SecD/SecF*	7.4286	43	13	36
10	USA300HOU_0126	Iron (Fe^{3+}) ABC transporter binding protein	*sirA*	6.4555	67	31	175
170	USA300HOU_2536	Secretory antigen	*Ssa*	6.3315	116	42	106
27	USA300HOU_0340	Triacylglycerol lipase	*lip1*	6.2055	62	75	21
122	USA300HOU_1802	Serine protease	*SplE*	6.0741	78	156	56
124	USA300HOU_1804	Serine protease	*SplC*	6.014	83	120	57
2	SAUSA300_1918	Beta hemolysin	*hlb*	5.8778	54	61	40
8	USA300HOU_0108	Phosphatidylinositol diacylglycerol-lyase	*plc*	5.7318	66	66	52
136	USA300HOU_1942	Cell surface protein	*MapW2*	5.4386	2	81	33
148	USA300HOU_2266	Iron (Fe^{3+}) ABC transporter binding protein	*fhuD2*	5.2362	36	40	65
177	USA300HOU_2644	*N*-Acetylmuramoyl-L-alanine amidase		5.2226	52	147	29
26	USA300HOU_0327	Acid phosphatase		5.1107	110	92	139
65	USA300HOU_0725	Putative hemolysin		4.9086	38	32	54
154	USA300HOU_2386	ABC transporter ATP-binding protein		4.6335	30	46	75
11	USA300HOU_0146	Cell wall surface anchor protein	*sasD*	4.3445	4	23	14
158	USA300HOU_2402	Gamma hemolysin component A	*hlgA*	4.3075	21	85	51
170	USA300HOU_2549	Carboxylate dehydrogenase	*rocA*	4.1521	37	16	26

[a]mRNA transcripts whose aggregate normalized median value fell in the top quartile (highest 47 of 188) of evaluated transcripts in pediatric SSTI are shown ranked from highest to lowest expression. Corresponding transcript number from the demonstrated heat maps are listed. Also shown are the ranks of each transcript's aggregate normalized median value in murine SSTI and nares at day 3 after infection and in USA300 cultured to mid-log growth phase in tryptic soy broth. Ranks indicate highest to lowest aggregate medians (from 1 to 188). Murine experiments included 9 or 10 animals per infection group and were repeated 2 to 4 times. Extraction of mRNA from *in vitro*-cultured USA300 was repeated 6 times for expression analysis.

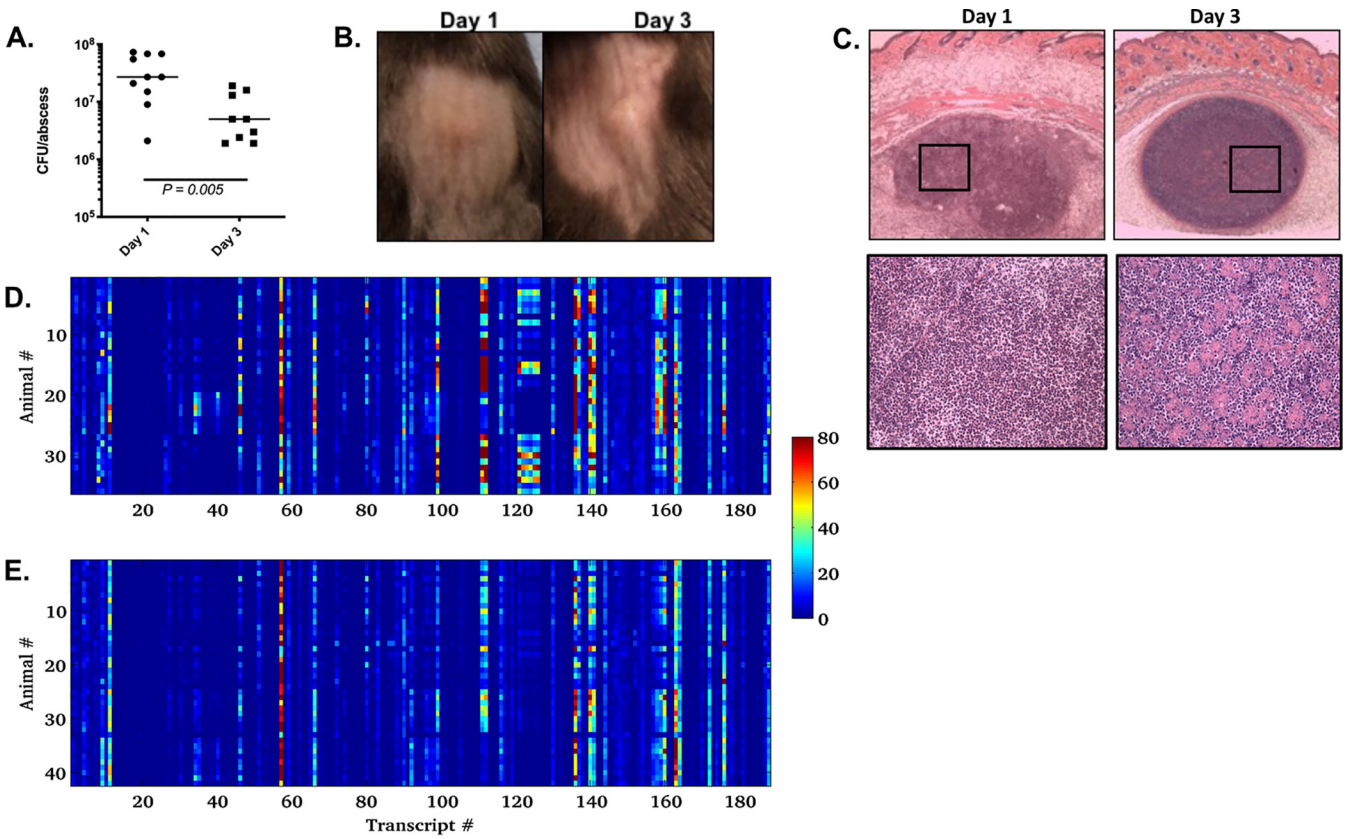

FIG 2 *S. aureus* transcript analysis in murine abscess model. Abscesses were excised from mice on days 1 and 3 after subcutaneous (s.c.) injection of 100 μl 5×10^5 to 1×10^6 CFU USA300-MR. CFU from abscess homogenates from each mouse (A) and representative images of lesions (B) are shown. (C) Hematoxylin and eosin (H&E)-stained cross-sections of abscesses (10× in top images) demonstrate neutrophil infiltration (squares at 40× in lower images) and progressive abscess encapsulation. (D and E) Heat map of 188 *S. aureus* mRNA transcripts (*x* axis) from murine abscess homogenate on day 1 (D) or day 3 (E) after infection. Raw transcript counts in each sample were normalized to the median target count for that sample. Experiments included 9 or 10 animals per infection group and were repeated 3 or 4 times. Mann-Whitney test of significance was used to evaluate difference in CFU.

models as well. It would be expected that *mecA* expression should significantly differ in abscesses caused by MRSA versus MSSA, and this finding further supports the validity of this expression analysis method. There is no obvious biological rationale that may explain why expression of a nickel/peptide transporter might differ except that this transcript has been described as one subunit of a complex that is unique to USA300 strains (24). No other parameters were significantly associated with any transcript expression levels once the model results were adjusted for FDR.

Analysis of mRNA signature in murine SSTI. Next we assessed the similarity of the *S. aureus* expression profile seen in pediatric abscesses to that in a mouse model of *S. aureus* soft tissue abscess. First, we demonstrated via controlled RNA-spiking experiments that the lower limit of bacterial abundance required in a sample to still allow robust *S. aureus* expression analysis using the developed methods was $\sim 1 \times 10^4$ CFU. We used a murine model of staphylococcal skin abscess that induces visible soft tissue abscess without dermonecrosis or bacterial dissemination by day 2 to 3; abscesses increase in size through day 5 to 7 and resolve spontaneously with or without drainage by day 14 postinfection (25, 26). Murine abscess homogenates were processed on days 1 ($n = 36$) and 3 ($n = 42$) after subcutaneous injection of 5×10^5 to 1×10^6 CFU USA300-MRSA and were found to contain sufficient bacterial CFU for analysis (median CFU on day 1 of 2.7×10^7 and on day 3 of 5×10^6; $P = 0.005$ [Fig. 2A]). The abscess phenotype was visible by day 1 and well defined by day 3 after infection (Fig. 2B), and histopathology of abscesses showed early neutrophil influx surrounding bacteria on day 1 and coalesced, well-contained abscess on day 3 after infection (Fig. 2C). The mRNA signatures from day 1 and day 3 murine abscesses shown in Fig. 2D and E revealed similar

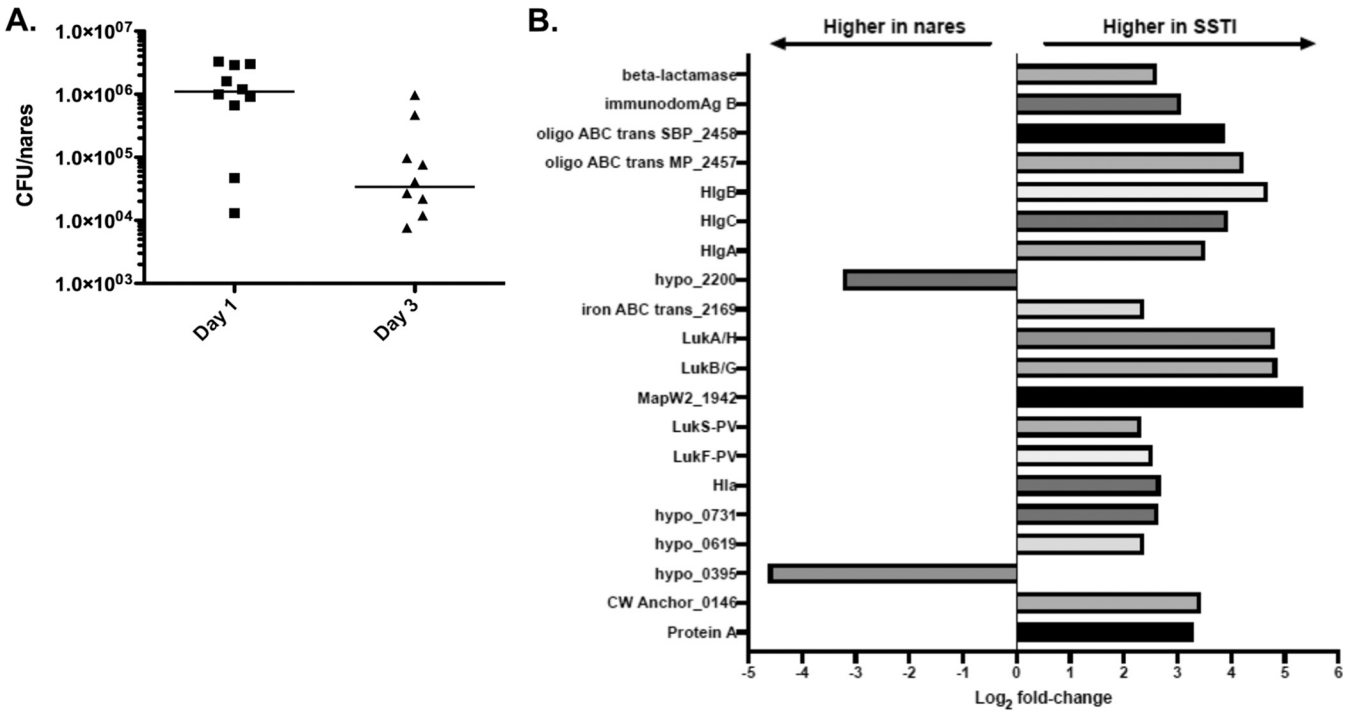

FIG 3 *S. aureus* expression in murine nasal colonization. Nares were harvested from mice on day 1 or 3 after intranasal inoculation of 10 μl of 1×10^7 CFU USA300-MR. CFU from filtrates of nasal homogenates from each mouse are shown (A). Normalized median mRNA transcript counts from RNA extracted from nares day 3 after colonization were compared to normalized median transcript counts from RNA extracted from day 3 murine SSTI and are shown as $\log_2$ fold change (B). Shown are the transcripts with normalized median expression of >10 in either nares or SSTI and $\log_2$ fold change of >2. Transcripts are identified by their symbol or locus ID within the published sequence for the infecting strain (USA300_TCH1516). Experiments included 9 or 10 animals per group and were repeated 2 to 4 times.

mRNA profiles. Similar to the case with pediatric SSTI, the mRNA profile from murine abscesses was consistent across animals. The transcript profiles from day 1 and day 3 abscesses demonstrated significant overlap, though some transcripts enriched in day 1 abscesses were uniformly lower in day 3 abscesses, consistent with a significant decrease in bacterial burden over time.

Transcript profile of *S. aureus* in nasal colonization. Several studies have demonstrated that *S. aureus* SSTI and other infections typically are caused by an individual's endogenous colonizing *S. aureus* strain (27–29); thus, knowledge of transcriptional changes that occur as *S. aureus* transitions from commensal to SSTI strain might identify proteins that facilitate this transition. Since the bacterial burden sampled from nasal swabs of our pediatric abscess patients was insufficient for NanoString evaluation, we developed a nasal colonization model in mice that yielded high enough bacterial burden at day 3 after inoculation (Fig. 3A) to allow *S. aureus* expression analysis directly from RNA extracted from murine nares. As shown in Fig. 3B, many of the *S. aureus* virulence factors with established roles in SSTI pathogenesis had ~1-log-fold higher expression in RNA extracted from murine SSTI at day 3 postinfection than in RNA from murine nares at day 3 postcolonization (e.g., *hla*, *LukS-PV* and *LukF-PV*, and *hlgB*, *-C*, and *-A*). There were additionally several mRNA transcripts that encode *S. aureus* proteins of "hypothetical" function that had >1-log-fold higher expression in either murine nasal colonization or SSTI. Proteins encoded by the genes that demonstrate substantial increase in expression from a colonization environment to the abscess environment may represent those critical to facilitating this transition and should be explored further for their role in SSTI pathogenicity.

Overlap of transcripts with enriched expression in both pediatric and murine infections. We next evaluated the overlap of transcripts that were in the top quartiles of expression in pediatric abscesses and the evaluated murine infections. Shown in Table 2 are the *S. aureus* mRNA transcripts with the highest median expression in

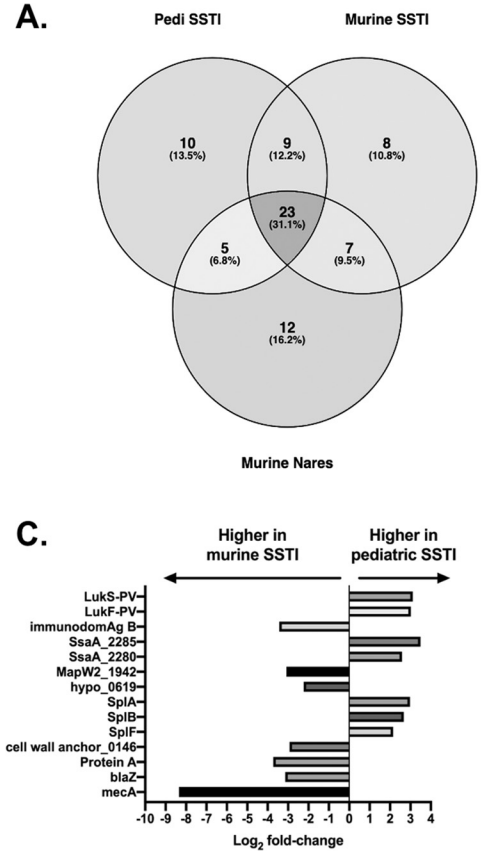

B.

Transcript number	Locus number in reference strain USA300_TCH1516	Encoded protein (Symbol)
112	USA300HOU_1431	Panton-Valentine leucocidin subunit S (LukS-PV)
111	USA300HOU_1430	Panton-Valentine leucocidin subunit F (LukF-PV)
172	USA300HOU_2564	Immunodominant Ag A (IsaA)
163	USA300HOU_2457	Oligopeptide ABC transporter membrane protein
99	USA300HOU_1099	Alpha hemolysin (Hla)
66	USA300HOU_0731	Hypothetical protein
137	USA300HOU_1946	Hypothetical protein
51	USA300HOU_0465	LysM family autolysin (Sle1)
90	USA300HOU_1007	Chitinase
57	USA300HOU_0619	Hypothetical protein
130	USA300HOU_1833	Peptidylprolyl isomerase (PrsA2)
83	USA300HOU_0939	Extracellular adherence protein (Eap)
59	USA300HOU_0651	ABC transporter ATP-binding protein (MntC)
88	USA300HOU_0997	Bifunctional autolysin (Atl)
144	USA300HOU_2169	Iron ABC transporter binding protein
119	USA300HOU_1725	Catabolite control protein A (CcpA)
46	USA300HOU_0437	Hypothetical protein
117	USA300HOU_1636	Bifunctional preprotein translocase subunit (SecD/F)
148	USA300HOU_2266	Iron ABC transporter binding protein (FhuD2)
65	USA300HOU_0725	Putative hemolysin
154	USA300HOU_2386	ABC transporter ATP-binding protein
11	USA300HOU_0146	cell wall surface anchor protein
170	USA300HOU_2549	carboxylate dehydrogenase

FIG 4 Highly expressed transcripts in pediatric SSTI, murine SSTI, and murine nasopharyngeal colonization. A Venn diagram of transcripts with aggregate normalized median values in the top quartile (47 of 188) from pediatric SSTI, murine SSTI, and murine nares is shown (A). The locus number from reference strain USA300_TCH1516 and annotated encoded protein description of each of the 23 transcripts in the intersection of all infection subsets are listed (B). Corresponding transcript numbers from the demonstrated heat maps are also listed. Also shown are the transcripts with normalized median expression of >10 in murine day 3 or pediatric SSTI and $\log_2$ fold change of >2 between these two conditions (C). Transcripts are identified by their symbol or locus ID within the published sequence for the infecting strain (USA300_TCH1516).

pediatric SSTI ranked from the highest to lowest (top quartile of those evaluated; $n = 47$ of 188). Also shown are the ranked transcript medians within the batched expression analysis data from murine SSTI and colonization day 3 postinfection, with 1 being the highest ranked transcript in each infection cohort. To illustrate the overlap between the genes that are highly expressed (top quartile) under each condition, we show a Venn diagram (Fig. 4A) including the list of transcripts that fall in the overlapping region of all 3 conditions (Fig. 4B). Enhanced expression of alpha hemolysin and the PVL subunits, while expected in SSTI, might not have been expected during colonization, but this may reflect the relatively high expression of these three genes across all sampled contexts, including during *in vitro* growth of *S. aureus* (Table 2). Meanwhile, expression of other cytolysins such as gamma hemolysin and leukocidin AB was increased only during SSTI. The ABC transporter subunits and proteins of unknown function whose expression was elevated across all measured infections deserve further investigation for their role in carriage and SSTI.

We also evaluated which transcripts were differentially expressed between pediatric and murine SSTI. We chose the day 3 murine SSTI data set to most closely resemble the timing of the sampled pediatric abscesses. Shown in Fig. 4C are the transcripts that were above background expression under both conditions but demonstrated at least ~1-log-fold difference between hosts. Several transcripts, such as *LukS-PV*, *LukF-PV*, and cell wall anchor protein transcripts *MapW2* and USA300HOU_0146, were in the top quartile of expression in both pediatric and murine SSTI but were substantially higher in one or the other. Transcripts for secretory antigens (*SsaA*) and serine

proteases (*SplA/B/F*) were uniquely enriched in human but not murine abscesses. Conversely, several transcripts associated with immune evasion and virulence (protein A and immunodominant antigen B [30, 31]) were highly expressed in murine but not human SSTI. Transcripts encoding beta-lactam resistance (*mecA* and *blaZ*) were enriched in murine SSTI compared to pediatric SSTI, but this may well be an artifact of the heterogeneity of infecting strains in the pediatric samples compared to the homogenous representation of a USA300 MRSA strain in murine infections.

DISCUSSION

To date, no candidate vaccine directed against *S. aureus* has shown consistent efficacy in clinical trials. Many potential explanations have been advanced for these failures, including antigen selection, questionable importance of the polysaccharide capsule 5 or 8 in disease, redundant mechanisms of pathogenesis, and, most broadly, a lack of understanding of the underlying mechanisms of immunity to *S. aureus*. In this study, we examined the expression level of *S. aureus* proteins in the context of infection and evaluated to what extent a mouse model of soft tissue infection predicts gene expression in human disease. Many of the transcripts encoding proteins with established associations or roles in abscess formation were enriched during human SSTI. For example, mRNA encoding the two subunits of PVL represented two of the highest expressed in our analysis in both MRSA and MSSA SSTI. While the role of this toxin in the pathogenesis of soft tissue infection remains controversial, PVL positivity by DNA analysis has been strongly associated with *S. aureus* SSTI and abscess formation (32) but not with more invasive staphylococcal infections (33). Our findings also demonstrated enrichment of mRNA encoding the pore-forming toxin alpha hemolysin (*hla*) in *S. aureus* SSTI. Animal models of SSTI using *hla*-deficient *S. aureus* strains have shown attenuation of the SSTI phenotype (20, 34), suggesting that *hla* may contribute to pathogenesis of staphylococcal SSTI. In addition to these antigens, transcripts encoding other toxins and cytolysins were well represented among the highest expressed genes in the subset studied. We also noted that many genes whose expression was enriched in our study encode proteins that elicited the highest convalescent antibody response in recent studies of IgG reactivity in patients recovering from *S. aureus* SSTI (35, 36), a finding compatible with their relatively high level of gene expression during human SSTI.

We also identified a number of transcripts encoding proteins of unknown function that are enriched in pediatric abscesses. Many of these uncharacterized proteins, along with several subunits of ABC transporter complexes, were highly expressed in pediatric abscesses and upregulated in murine abscesses compared to murine nasal carriage. In addition to being a highly virulent organism in certain situations, *S. aureus* is also a successful commensal organism, colonizing between 20 and 40% of humans at any one time. Therefore, therapeutic and preventive approaches that target proteins well expressed during both colonization and infection might have the highest likelihood of success. Thus, further analysis of the function of these proteins and whether they contribute to fitness in colonization and/or virulence may point to novel *S. aureus* targets.

A limitation encountered in this study was that only ~1/3 of samples from *S. aureus* abscesses yielded sufficient quality RNA for analysis. Additionally, there is the technical limitation to the number of transcripts that can be evaluated in a single reaction, thereby preventing evaluation of the entire bacterial transcriptome. However, the streamlined sample processing and analysis steps and high-throughput expression analysis make large studies of human infection samples more feasible. Furthermore, since the specificity of this analysis relies solely on that of the hybridization primers, host and bacterial transcript analyses can be carried out in the same hybridization. We are currently evaluating this approach in human infection samples to better assess the effect of the host immune response on bacterial expression, as has been suggested in an animal model of invasive *S. aureus* infection (37).

Our study builds on previous efforts to examine *in vivo* expression profiles. Previously published studies investigating *S. aureus* gene expression in human SSTI

evaluated a small number of clonal (USA300) infection samples using microarray analysis (38) or a smaller number of preselected genes using reverse transcription-PCR (qRT-PCR) (39). These studies demonstrated increased expression of known toxins such as alpha hemolysin, PVL, and gamma hemolysin subunits. In addition to its larger sample size, our work represents a broad range of infecting strains and sequence types of *S. aureus*, sampled at various times of clinical presentation, with or without the concomitant use of oral antibiotics. We show a relative overall stability of the mRNA signature profile across pediatric samples, suggesting that gene expression by *S. aureus* within a soft tissue abscess cavity is reasonably conserved, despite differential exposure to host responses or antibiotics (40).

Another important finding from our work is the vast difference in the *S. aureus* expression profile from *in vivo* human infection compared to that of the infecting strains regrown *in vitro*. Such differences have been corroborated in murine staphylococcal pneumonia (41) and further support the importance of bacterial expression analysis from human infection samples rather than from strain libraries (42).

Our work also highlights important considerations for selection of *S. aureus* antigens as targets for prevention or treatment of infection. Perhaps one of the most relevant challenges to the development of an effective staphylococcal vaccine is our incomplete understanding of mechanisms of immunity to staphylococcal infections (43, 44). Another longstanding obstacle is that the performance of vaccine candidates in animal models has not been predictive of success in human trials (45, 46), suggesting that animal models do not accurately recapitulate staphylococcal infections in humans. Potential reasons for this include host species differences in niche-specific immune responses and expression of receptors for bacterial ligands (47) and differing microbiomes that might drive interference or enhancement of staphylococcal pathogenesis (48, 49). Another factor that may contribute to the poor predictive value of animal models for efficacy of subunit vaccine candidates in humans is interspecies differences in the expression of the vaccine antigens during infection.

In this study, we developed a murine SSTI model that phenotypically and histologically recapitulates human SSTI, and while there was significant overlap of the *S. aureus* expression profiles from pediatric and murine SSTI, there were some transcripts whose expression differed significantly between the species. For example, transcripts for several of the serine protease-like proteins that were enriched in pediatric SSTI were not enriched in murine SSTI by day 3 postinfection (*splA* to *-E*; transcript numbers 122 to 126 on corresponding heat maps in Fig. 1A, Fig. 2E, and Fig. 4C); thus, if relying on studies from animal infection alone to identify bacterial genes upregulated *in vivo*, these would likely be missed. And conversely, the gene encoding immunodominant antigen B (*isaB*) was highly expressed in murine abscesses, but not in human abscesses (Table S2). Mouse models have been used to demonstrate a role for *isaB* in *S. aureus*-mediated skin inflammation (50), but our findings suggest diminished expression of *isaB* in human abscesses; whether there is a difference in *isaB* expression in earlier phases of human skin infection is unknown.

Application of these findings to subunit vaccine antigens that have been tested for efficacy in human trials may provide clues as to why they failed. For example, iron-regulated surface determinant protein B (*isdB*), a single-antigen investigational vaccine that failed to prevent invasive *S. aureus* infection in patients undergoing elective cardiothoracic surgery (51), had relatively low expression in pediatric SSTI (rank 111 of 188 transcripts [Table S2]). While there may be other reasons for this failure, relatively low expression of *isdB* in human soft tissue infection could explain why the vaccine failed. Taken together, these findings demonstrate the importance of evaluating the expression of *S. aureus* genes *in vivo* during human infection to fully understand their potential as vaccine candidates, rather than relying on animal model data alone.

MATERIALS AND METHODS

Study enrollment and sample collection. Enrolled subjects were otherwise healthy patients under the age of 21 with an abscess requiring drainage who presented to the Emergency Department at

Boston Children's Hospital between September 2013 and December 2016. Exclusion criteria included an infection associated with either prior surgery or indwelling foreign material, immunocompromised status, or presentation with signs of severe illness such as hemodynamic compromise. Informed consent was obtained from all enrolled subjects, and the study protocol was approved by the Boston Children's Hospital Institutional Review Board. Purulent drainage was cultured as per standard routine of care, and two additional swabs (FLOQswabs; Copan Flock Technologies, Italy) of drainage were collected, and submerged into 1 ml RNA Protect Bacteria (Qiagen Inc., Germantown, MD), and stored at −20°C until further processing. For abscesses microbiologically confirmed as due to *S. aureus*, isolates were collected from the BCH Clinical Microbiology Laboratory, regrown for 3 h in tryptic soy broth (TSB), and stored as 20% glycerol stocks at −80°C. DNA from each clinical strain was isolated and prepared for multilocus sequence typing performed by ID Genomics.

Sample processing and RNA extraction. Stored samples from patients with *S. aureus* abscesses were thawed. Swabs were removed, placed into a 15-ml tube containing 1 ml fresh RNA Protect Bacteria, and vigorously vortexed for 1 min. Swabs were discarded. RNA Protect Bacteria from the original sample tube and from swab tube was transferred to fresh microcentrifuge tubes and centrifuged at 13,000 rpm for 5 min. Pellets were resuspended in 0.5 ml RNase-free phosphate-buffered saline (PBS; Ambion, Thermo Fisher Scientific) containing 0.05% Triton X-100 (Acros Organics; Thermo Fisher Scientific) and 10 U/ml RNase inhibitor (RNAseIn Plus; Promega, Madison, WI). Contents from both tubes were combined into round-bottom tubes, incubated at room temperature for 10 min, and homogenized for 30 s using a Tissue-Tearor. The homogenate was transferred to a fresh microcentrifuge tube and pelleted. Pellets were resuspended in 500 μl lysis buffer containing 30 mM Tris/1 mM EDTA, 0.01 U/μl RNase inhibitor, 5 mg/ml lysostaphin (Sigma-Aldrich, St. Louis, MO), and 0.1 mg/ml proteinase K (Qiagen). After a 30-min incubation at 37°C with vortexing every 5 min, 350 μl buffer RLT was added and RNA extraction was carried out as per protocol using RNeasy kits (Qiagen). For *S. aureus* isolates regrown *in vitro*, 1 ml culture grown in TSB to an optical density at 600 nm (OD_{600}) of 0.6 to 0.7 was pelleted and resuspended in RNA Protect Bacteria and then pelleted and lysed as described above. Extracted RNA samples were stored at −80°C until used for expression analysis.

Animal studies. All animal studies were approved by the Boston Children's Hospital Animal Care and Use Committee.

Murine SSTI model. All infections in mice were carried out in female C57BL/6 mice aged 4 to 6 weeks from Jackson Laboratories (Bar Harbor, ME). The strain used to infect mice in the abscess model was USA300TCH1516 (MRSA; ATCC BAA-1717). Inocula were prepared fresh for each experiment by back-dilution of an overnight culture as previously described (52). Under gentle restraint, the hind dorsum was shaved with electric clippers and injected subcutaneously with 5×10^5 to 1×10^6 bacteria/100 μl via 27G needle. Abscesses were excised from euthanized mice and placed in either 1 ml sterile PBS (for CFU enumeration) or RNA Protect Bacteria (for RNA extraction). Infected murine tissue was homogenized using a Tissue-Tearor. The homogenate was passed through a 30-μm filter, after which the filtrate was either plated for determination of CFU recovery or pelleted and resuspended in lysis buffer for further RNA extraction as described above for clinical samples.

Murine nasal colonization model. The same bacterial strain as used in the murine SSTI model was similarly prepared to infect mice intranasally to establish nasal carriage. For colonization challenge, mice were gently restrained in a 50-ml conical tube with the narrow end removed to expose the nares. Mice were inoculated intranasally with 1×10^7 bacteria/10 μl. Mice were euthanized at 1 or 3 days after colonization, and nares were excised and homogenized, filtered, and plated as described above for enumeration of the CFU burden of colonization. For RNA extraction, nares were placed in 15-ml conical tubes containing 1 ml Tri reagent (Sigma; item number 93289). Tubes were vortexed at maximum speed for 1 min each, and then the supernatant was collected and transferred into 2-ml screw-top tubes. A 200-μl volume of glass beads (acid washed, $<$106 μm) was added to each tube and then disrupted using a bead beater, 5 times total for 1 min each, letting tubes rest on ice for 1 min in between. A 200-μl volume of chloroform was added, and tubes were vortexed and spun at 4°C for 15 min at 12,000 $\times$ *g*. The aqueous phase (top layer) was transferred to a 1-ml tube, and 3 M sodium acetate was added at 1/10 volume with 2.5$\times$ volume of cold 100% ethanol. After thorough mixing, samples were kept at −80°C overnight. The next day, samples were pelleted at 4°C for 15 min at 12,000 $\times$ *g* and pellets were washed twice with 500 μl 70% ethanol. Dried pellets were dissolved in 15 μl RNase-free water and stored at −80°C.

Expression analysis. Primers for the 169 genes with a signal sequence for secretion or surface expression and for 23 additional genes of interest were designed using reference genome sequence *Staphylococcus aureus* USA300_TCH1516, NCBI taxon identifier (ID) 451516 at https://img.jgi.doe.gov/; primer sequences are listed in Table S1. Only genes with $>$95% homology across published *S. aureus* sequences were included. In design of the primers, areas of homology with human and murine genes or with *Staphylococcus epidermidis* were avoided using *in silico* analysis. RNA (12 μl total RNA from each abscess sample) was hybridized for 23 h at 65°C with primer sets and NanoString Elements reagents (30-μl total volume of each hybridization). Hybridized samples were washed and immobilized onto cartridges (NanoString prep station) that were analyzed (digital analyzer) for direct counting of the fluorescent molecular barcodes unique to each primer that attach to hybridized transcript within each flow cell. Data from a sample were considered evaluable if the raw transcript counts across a sample displayed a varied range of 1 to a minimum of 1×10^4.

Statistical analysis. All statistical modeling and analyses and heat map generation were conducted using the software Matlab (Mathworks, Inc.). Data presented in tables and figures were normalized to their individual medians (over all transcripts) or their individual/batch inoculum (also normalized to their respective medians). Statistical analysis of pediatric expression data as a function of clinical

characteristics was conducted using ordinary linear regression models. Separate models were developed for individual transcripts, with expression level as the continuous outcome and different combinations of independent variables, including patient age, methicillin susceptibility, patient gender, days of symptoms, history of prior abscesses, and whether patients were on antibiotics at time of sample acquisition. Given that a large number of models were tested (separate models for each individual transcript), all *P* values for the regression coefficients of interest were adjusted for the false-discovery rate using a well-established approach (23). Other analyses and graphs were generated using Prism (GraphPad Software, Inc.). Venn diagrams were generated using Venny 2.1.0 (https://bioinfogp.cnb.csic.es/tools/venny/index.html).

SUPPLEMENTAL MATERIAL

Supplemental material is available online only.

SUPPLEMENTAL FILE 1, PDF file, 1 MB.

SUPPLEMENTAL FILE 2, XLSX file, 0.02 MB.

SUPPLEMENTAL FILE 3, XLSX file, 0.02 MB.

ACKNOWLEDGMENTS

We thank the patients who participated in this study and the Boston Children's Hospital Emergency Department staff and Research Coordinator Program. We acknowledge the Harvard Digestive Diseases Center at BCH and Rami Burstein at the Beth Israel Deaconess Medical Center for use of the NanoString platform equipment.

K.M. acknowledges funding support from the Charles Hood Foundation and the BCH Translational Research Program. This work was conducted in part with support from Harvard Catalyst (to C.S.), The Harvard Clinical and Translational Science Center (National Center for Advancing Translational Sciences, National Institutes of Health award UL 1TR002541), and financial contributions from Harvard University and its affiliated academic health care centers.

The content is solely the responsibility of the authors and does not necessarily represent the official views of Harvard Catalyst, Harvard University and its affiliated academic health care centers, or the National Institutes of Health.

REFERENCES

1. Talan DA, Krishnadasan A, Gorwitz RJ, Fosheim GE, Limbago B, Albrecht V, Moran GJ, EMERGEncy ID Net Study Group. 2011. Comparison of Staphylococcus aureus from skin and soft-tissue infections in US emergency department patients, 2004 and 2008. Clin Infect Dis 53:144–149. https://doi.org/10.1093/cid/cir308.
2. Pallin DJ, Egan DJ, Pelletier AJ, Espinola JA, Hooper DC, Camargo CA, Jr. 2008. Increased US emergency department visits for skin and soft tissue infections, and changes in antibiotic choices, during the emergence of community-associated methicillin-resistant Staphylococcus aureus. Ann Emerg Med 51:291–298. https://doi.org/10.1016/j.annemergmed.2007.12.004.
3. Karamatsu ML, Thorp AW, Brown L. 2012. Changes in community-associated methicillin-resistant Staphylococcus aureus skin and soft tissue infections presenting to the pediatric emergency department: comparing 2003 to 2008. Pediatr Emerg Care 28:131–135. https://doi.org/10.1097/PEC.0b013e318243fa36.
4. Broker BM, Holtfreter S, Bekeredjian-Ding I. 2014. Immune control of Staphylococcus aureus—regulation and counter-regulation of the adaptive immune response. Int J Med Microbiol 304:204–214. https://doi.org/10.1016/j.ijmm.2013.11.008.
5. Alonzo F, III, Torres VJ. 2013. Bacterial survival amidst an immune onslaught: the contribution of the Staphylococcus aureus leukotoxins. PLoS Pathog 9:e1003143. https://doi.org/10.1371/journal.ppat.1003143.
6. Dinges MM, Orwin PM, Schlievert PM. 2000. Exotoxins of Staphylococcus aureus. Clin Microbiol Rev 13:16–34. https://doi.org/10.1128/CMR.13.1.16.
7. Proctor RA. 2012. Challenges for a universal Staphylococcus aureus vaccine. Clin Infect Dis 54:1179–1186. https://doi.org/10.1093/cid/cis033.
8. Daum RS, Spellberg B. 2012. Progress toward a Staphylococcus aureus vaccine. Clin Infect Dis 54:560–567. https://doi.org/10.1093/cid/cir828.
9. Westermann AJ, Barquist L, Vogel J. 2017. Resolving host-pathogen interactions by dual RNA-seq. PLoS Pathog 13:e1006033. https://doi.org/10.1371/journal.ppat.1006033.
10. Casneuf T, Van de Peer Y, Huber W. 2007. In situ analysis of cross-hybridisation on microarrays and the inference of expression correlation. BMC Bioinformatics 8:461. https://doi.org/10.1186/1471-2105-8-461.
11. Kukurba KR, Montgomery SB. 2015. RNA sequencing and analysis. Cold Spring Harb Protoc 2015:951–969. https://doi.org/10.1101/pdb.top084970.
12. Minshall N, Git A. 2020. Enzyme- and gene-specific biases in reverse transcription of RNA raise concerns for evaluating gene expression. Sci Rep 10:8151. https://doi.org/10.1038/s41598-020-65005-0.
13. Geiss GK, Bumgarner RE, Birditt B, Dahl T, Dowidar N, Dunaway DL, Fell HP, Ferree S, George RD, Grogan T, James JJ, Maysuria M, Mitton JD, Oliveri P, Osborn JL, Peng T, Ratcliffe AL, Webster PJ, Davidson EH, Hood L, Dimitrov K. 2008. Direct multiplexed measurement of gene expression with color-coded probe pairs. Nat Biotechnol 26:317–325. https://doi.org/10.1038/nbt1385.
14. Tenover FC, Goering RV. 2009. Methicillin-resistant Staphylococcus aureus strain USA300: origin and epidemiology. J Antimicrob Chemother 64:441–446. https://doi.org/10.1093/jac/dkp241.
15. Diep BA, Gill SR, Chang RF, Phan TH, Chen JH, Davidson MG, Lin F, Lin J, Carleton HA, Mongodin EF, Sensabaugh GF, Perdreau-Remington F. 2006. Complete genome sequence of USA300, an epidemic clone of community-acquired meticillin-resistant Staphylococcus aureus. Lancet 367:731–739. https://doi.org/10.1016/S0140-6736(06)68231-7.
16. Barczak AK, Gomez JE, Kaufmann BB, Hinson ER, Cosimi L, Borowsky ML, Onderdonk AB, Stanley SA, Kaur D, Bryant KF, Knipe DM, Sloutsky A, Hung DT. 2012. RNA signatures allow rapid identification of pathogens and antibiotic susceptibilities. Proc Natl Acad Sci U S A 109:6217–6222. https://doi.org/10.1073/pnas.1119540109.
17. Tekletsion YK, Christensen H, Finn A. 2018. Gene detection and expression profiling of Neisseria meningitidis using NanoString nCounter platform. J Microbiol Methods 146:100–103. https://doi.org/10.1016/j.mimet.2018.02.003.

18. Lacey KA, Geoghegan JA, McLoughlin RM. 2016. The role of Staphylococcus aureus virulence factors in skin infection and their potential as vaccine antigens. Pathogens 5:22. https://doi.org/10.3390/pathogens5010022.
19. Olaniyi RO, Pancotto L, Grimaldi L, Bagnoli F. 2018. Deciphering the pathological role of staphylococcal alpha-toxin and Panton-Valentine leukocidin using a novel ex vivo human skin model. Front Immunol 9:951. https://doi.org/10.3389/fimmu.2018.00951.
20. Kennedy AD, Bubeck Wardenburg J, Gardner DJ, Long D, Whitney AR, Braughton KR, Schneewind O, DeLeo FR. 2010. Targeting of alpha-hemolysin by active or passive immunization decreases severity of USA300 skin infection in a mouse model. J Infect Dis 202:1050–1058. https://doi.org/10.1086/656043.
21. Kobayashi SD, Malachowa N, DeLeo FR. 2015. Pathogenesis of Staphylococcus aureus abscesses. Am J Pathol 185:1518–1527. https://doi.org/10.1016/j.ajpath.2014.11.030.
22. Singh R, Ray P. 2014. Quorum sensing-mediated regulation of staphylococcal virulence and antibiotic resistance. Future Microbiol 9:669–681. https://doi.org/10.2217/fmb.14.31.
23. Benjamini Y, Hochberg Y. 1995. Controlling the false discovery rate: a practical and powerful approach to multiple testing. J R Stat Soc 57:289–300. https://doi.org/10.1111/j.2517-6161.1995.tb02031.x.
24. Liang C, Schaack D, Srivastava M, Gupta SK, Sarukhanyan E, Giese A, Pagels M, Romanov N, Pane-Farre J, Fuchs S, Dandekar T. 2016. A Staphylococcus aureus proteome overview: shared and specific proteins and protein complexes from representative strains of all three clades. Proteomes 4:8. https://doi.org/10.3390/proteomes4010008.
25. Zhang F, Jun M, Ledue O, Herd M, Malley R, Lu YJ. 2017. Antibody-mediated protection against Staphylococcus aureus dermonecrosis and sepsis by a whole cell vaccine. Vaccine 35:3834–3843. https://doi.org/10.1016/j.vaccine.2017.05.085.
26. Kim HK, Missiakas D, Schneewind O. 2014. Mouse models for infectious diseases caused by Staphylococcus aureus. J Immunol Methods 410:88–99. https://doi.org/10.1016/j.jim.2014.04.007.
27. Huang YC, Chou YH, Su LH, Lien RI, Lin TY. 2006. Methicillin-resistant Staphylococcus aureus colonization and its association with infection among infants hospitalized in neonatal intensive care units. Pediatrics 118:469–474. https://doi.org/10.1542/peds.2006-0254.
28. Valentine FC, Hall-Smith SP. 1952. Superficial staphylococcal infection. Lancet ii:351–354. https://doi.org/10.1016/S0140-6736(52)92245-9.
29. von Eiff C, Becker K, Machka K, Stammer H, Peters G. 2001. Nasal carriage as a source of Staphylococcus aureus bacteremia. Study group. N Engl J Med 344:11–16. https://doi.org/10.1056/NEJM200101043440102.
30. Falugi F, Kim HK, Missiakas DM, Schneewind O. 2013. Role of protein A in the evasion of host adaptive immune responses by Staphylococcus aureus. mBio 4:e00575-13. https://doi.org/10.1128/mBio.00575-13.
31. Mackey-Lawrence NM, Jefferson KK. 2013. Regulation of Staphylococcus aureus immunodominant antigen B (IsaB). Microbiol Res 168:113–118. https://doi.org/10.1016/j.micres.2012.07.003.
32. Barrios Lopez M, Gomez Gonzalez C, Orellana MA, Chaves F, Rojo P. 2013. Staphylococcus aureus abscesses: methicillin-resistance or Panton-Valentine leukocidin presence? Arch Dis Child 98:608–610. https://doi.org/10.1136/archdischild-2012-302695.
33. Shallcross LJ, Fragaszy E, Johnson AM, Hayward AC. 2013. The role of the Panton-Valentine leucocidin toxin in staphylococcal disease: a systematic review and meta-analysis. Lancet Infect Dis 13:43–54. https://doi.org/10.1016/S1473-3099(12)70238-4.
34. Kobayashi SD, Malachowa N, Whitney AR, Braughton KR, Gardner DJ, Long D, Bubeck Wardenburg J, Schneewind O, Otto M, Deleo FR. 2011. Comparative analysis of USA300 virulence determinants in a rabbit model of skin and soft tissue infection. J Infect Dis 204:937–941. https://doi.org/10.1093/infdis/jir441.
35. Pelzek AJ, Shopsin B, Radke EE, Tam K, Ueberheide BM, Fenyo D, Brown SM, Li Q, Rubin A, Fulmer Y, Chiang WK, Hernandez DN, Bannoudi HE, Sause WE, Sommerfield A, Thomsen IP, Miller AO, Torres VJ, Silverman GJ. 2018. Human memory B cells targeting Staphylococcus aureus exotoxins are prevalent with skin and soft tissue infection. mBio 9:e02125-17. https://doi.org/10.1128/mBio.02125-17.
36. Radke EE, Brown SM, Pelzek AJ, Fulmer Y, Hernandez DN, Torres VJ, Thomsen IP, Chiang WK, Miller AO, Shopsin B, Silverman GJ. 2018. Hierarchy of human IgG recognition within the Staphylococcus aureus immunome. Sci Rep 8:13296. https://doi.org/10.1038/s41598-018-31424-3.
37. Thanert R, Goldmann O, Beineke A, Medina E. 2017. Host-inherent variability influences the transcriptional response of Staphylococcus aureus during in vivo infection. Nat Commun 8:14268. https://doi.org/10.1038/ncomms14268.
38. Date SV, Modrusan Z, Lawrence M, Morisaki JH, Toy K, Shah IM, Kim J, Park S, Xu M, Basuino L, Chan L, Zeitschel D, Chambers HF, Tan MW, Brown EJ, Diep BA, Hazenbos WL. 2014. Global gene expression of methicillin-resistant Staphylococcus aureus USA300 during human and mouse infection. J Infect Dis 209:1542–1550. https://doi.org/10.1093/infdis/jit668.
39. Loughman JA, Fritz SA, Storch GA, Hunstad DA. 2009. Virulence gene expression in human community-acquired Staphylococcus aureus infection. J Infect Dis 199:294–301. https://doi.org/10.1086/595982.
40. Hodille E, Rose W, Diep BA, Goutelle S, Lina G, Dumitrescu O. 2017. The role of antibiotics in modulating virulence in Staphylococcus aureus. Clin Microbiol Rev 30:887–917. https://doi.org/10.1128/CMR.00120-16.
41. Chaffin DO, Taylor D, Skerrett SJ, Rubens CE. 2012. Changes in the Staphylococcus aureus transcriptome during early adaptation to the lung. PLoS One 7:e41329. https://doi.org/10.1371/journal.pone.0041329.
42. Pragman AA, Schlievert PM. 2004. Virulence regulation in Staphylococcus aureus: the need for in vivo analysis of virulence factor regulation. FEMS Immunol Med Microbiol 42:147–154. https://doi.org/10.1016/j.femsim.2004.05.005.
43. Bagnoli F, Bertholet S, Grandi G. 2012. Inferring reasons for the failure of Staphylococcus aureus vaccines in clinical trials. Front Cell Infect Microbiol 2:16. https://doi.org/10.3389/fcimb.2012.00016.
44. Proctor RA. 2019. Immunity to Staphylococcus aureus: implications for vaccine development. Microbiol Spectr 7:GPP3-0037-2018. https://doi.org/10.1128/microbiolspec.GPP3-0037-2018.
45. Fowler VG, Jr, Proctor RA. 2014. Where does a Staphylococcus aureus vaccine stand? Clin Microbiol Infect 20(Suppl 5):66–75. https://doi.org/10.1111/1469-0691.12570.
46. Pozzi C, Olaniyi R, Liljeroos L, Galgani I, Rappuoli R, Bagnoli F. 2017. Vaccines for Staphylococcus aureus and target populations. Curr Top Microbiol Immunol 409:491–528. https://doi.org/10.1007/82_2016_54.
47. Salgado-Pabon W, Schlievert PM. 2014. Models matter: the search for an effective Staphylococcus aureus vaccine. Nat Rev Microbiol 12:585–591. https://doi.org/10.1038/nrmicro3308.
48. Boldock E, Surewaard BGJ, Shamarina D, Na M, Fei Y, Ali A, Williams A, Pollitt EJG, Szkuta P, Morris P, Prajsnar TK, McCoy KD, Jin T, Dockrell DH, van Strijp JAG, Kubes P, Renshaw SA, Foster SJ. 2018. Human skin commensals augment Staphylococcus aureus pathogenesis. Nat Microbiol 3:881–890. https://doi.org/10.1038/s41564-018-0198-3.
49. Piewngam P, Zheng Y, Nguyen TH, Dickey SW, Joo HS, Villaruz AE, Glose KA, Fisher EL, Hunt RL, Li B, Chiou J, Pharkjaksu S, Khongthong S, Cheung GYC, Kiratisin P, Otto M. 2018. Pathogen elimination by probiotic Bacillus via signalling interference. Nature 562:532–537. https://doi.org/10.1038/s41586-018-0616-y.
50. Liu PF, Cheng JS, Sy CL, Huang WC, Yang HC, Gallo RL, Huang CM, Shu CW. 2015. IsaB inhibits autophagic flux to promote host transmission of methicillin-resistant Staphylococcus aureus. J Invest Dermatol 135:2714–2722. https://doi.org/10.1038/jid.2015.254.
51. Fowler VG, Allen KB, Moreira ED, Moustafa M, Isgro F, Boucher HW, Corey GR, Carmeli Y, Betts R, Hartzel JS, Chan IS, McNeely TB, Kartsonis NA, Guris D, Onorato MT, Smugar SS, DiNubile MJ, Sobanjo-ter Meulen A. 2013. Effect of an investigational vaccine for preventing Staphylococcus aureus infections after cardiothoracic surgery: a randomized trial. JAMA 309:1368–1378. https://doi.org/10.1001/jama.2013.3010.
52. Montgomery CP, Daniels M, Zhao F, Alegre ML, Chong AS, Daum RS. 2014. Protective immunity against recurrent Staphylococcus aureus skin infection requires antibody and interleukin-17A. Infect Immun 82:2125–2134. https://doi.org/10.1128/IAI.01491-14.